Journal of Sound and Vibration (2002) **255**(4), 763–775
doi:10.1006/jsvi.2001.4196, available online at http://www.idealibrary.com on IDEAL®

DAMPING OPTIMIZATION BY INTEGRATING ENHANCED ACTIVE CONSTRAINED LAYER AND ACTIVE-PASSIVE HYBRID CONSTRAINED LAYER TREATMENTS

Y. LIU

Maxtor Corporation, 500 *McCarthy Blvd.*, *Milpitas*, *CA* 95035, *U.S.A.*
E-mail: *Yanning_Liu@maxtor.com*

AND

K. W. WANG

Structural Dynamics and Controls Laboratory, *The Pennsylvania State University*, *University Park*, *PA* 16802-1412, *U.S.A. E-mail*: *kwwang@psu.edu*

(*Received* 14 *February* 2001, *and in final form* 27 *November* 2001)

The feasibility of integrating the enhanced active constrained layer (EACL) and active–passive hybrid constrained layer (HCL) treatments to achieve a better combination of the system's closed-loop damping and open-loop (fail-safe) damping (without active action) is investigated in this research. Given a uniform strain field in the host structure, the EACL with stiff and equal edge elements (symmetric EACL) has been shown to provide high closed-loop damping by significantly increasing the direct active control authority of the cover sheet. The open-loop damping of the system, however, could be low. On the other hand, the HCL has been demonstrated to offer more balanced open-loop and closed-loop damping actions, although the HCL closed-loop damping is not as high as that of the EACL. The idea here is therefore to combine the two approaches and develop an integrated HCL–EACL treatment. The focus is to maximize the system closed-loop damping while maintaining an open-loop damping margin for fail-safe reasons. For a given strain field in the host structure, optimization routines are used to search for the best design parameters: the optimal control gain, the stiffness of the edge elements and the active material coverage ratio in the constraining layer. It is found that integrating the EACL and the HCL will introduce more flexibility in the design of constrained layer damping treatments with actively enhanced actions. Higher open-loop damping can be achieved for the same closed-loop damping requirement and *vice versa*. The hybrid cover sheet is found to create significant shear in the viscoelastic layer while the edge elements are used to provide strong direct active control authority for the constraining layer. A better mixture of the open-loop and closed-loop damping can generally be obtained with the integrated system.

1. BACKGROUND

Active constrained layer (ACL) is a treatment that can provide both closed-loop and open-loop damping (fail-safe damping with no active effects) actions [1–3]. Such a system generally comprises a layer of viscoelastic material (VEM) sandwiched between a host structure and an active cover sheet, such as a piezoelectric layer. The active constraining layer can create active shear in the VEM as well as apply direct control action to the host structure. When the active action fails, the constraining layer behaves passively and can still

0022-460X/02/$35.00

restrain the VEM layer to create shear deformation as the host structure vibrates. In such a situation, the system becomes essentially a passive constrained layer (PCL) configuration. To provide the best ACL damping (combined open-loop and closed-loop damping effects), sequential optimization procedures [1, 4, 5] have been developed to maximize the open-loop damping for robustness or fail-safe properties and to maximize the closed-loop damping for vibration suppression performance.

While the optimized ACL treatments have been shown to provide promising results, two shortcomings associated with the ACL configuration have been observed. Compared to a purely active system where the piezoelectric actuator is directly bonded to a host structure, the direct active authority of the ACL device was found to be much lower [6, 7]. Compared to some passive materials, such as steel, the piezoelectric layer was found to be less effective in constraining the VEM layer [8–10]. Consequently, the open-loop damping of an optimally designed ACL system could still be less than that of a PCL treatment [10].

Because of these shortcomings of the current ACL configuration, new hybrid damping designs have been proposed. To increase the active control authority of the piezo-actuator in the ACL, an enhanced active constrained layer (EACL) concept [7] and separated active and passive designs [8, 9] have been suggested. To improve the constraining ability of the cover sheet in the ACL, an active–passive hybrid constrained layer (HCL) configuration has been explored [10]. For the self-contained EACL and HCL, the system open-loop and closed-loop damping contributions can be adjusted by changing various system parameters.

A generic study of the EACL [11] demonstrated that, for a symmetric strain field in the host structure, a symmetric EACL with stiff edge elements can significantly increase the closed-loop damping of an ACL but could reduce the system open-loop damping. However, it was also shown that a reasonable amount of closed-loop damping could still be obtained without reducing the open-loop damping by using an asymmetric EACL. In fact, different open-loop and closed-loop damping combinations can be achieved by adjusting the edge element stiffness.

The introduction of the HCL [10] provided another means of tuning the open-loop and closed-loop damping actions. The beauty of the HCL is that both the open-loop damping and closed-loop damping can be higher than that of the ACL by selecting a stiffer passive constraining material and designing appropriate active material coverage ratios. However, the closed-loop damping improvement of the HCL over the ACL is not as high as that of the EACL.

2. PROBLEM STATEMENTS AND RESEARCH OBJECTIVES

The ultimate goal of an active–passive hybrid damping treatment, such as ACL, EACL or HCL, is to provide a system with the highest possible closed-loop (combined active and passive actions) and open-loop (fail-safe property with no active controls) damping actions. In reality, however, these two needs usually result in contradictory requirements in design parameters. For example, to suppress vibration of a host structure with a uniform strain field, the highest closed-loop damping will require a symmetric EACL with stiff edge elements, which results in small open-loop damping. Similarly, in an HCL system, selecting a stiff passive constraining material and the optimal active material coverage ratio to maximize the closed-loop damping means that the system open-loop damping will be less than that of a PCL treatment with the same passive constraining material. Because of the conflicting requirements on the design parameters, one philosophy is to design the treatments for the maximum closed-loop damping while maintaining

a fail-safe margin (open-loop damping), which is essentially a constrained optimization problem.

Since the edge elements (in the EACL) and the active–passive hybrid constraining layer (in the HCL) can both be used to adjust the balance between the open-loop and closed-loop damping, it is possible that a better combination of the system total damping (closed-loop) and fail-safe damping (open-loop) can be obtained by integrating the EACL and HCL. Therefore, the objective of this research is to examine the feasibility of such an integration and to provide understanding of the characteristics of the integrated HCL–EACL system.

3. SYSTEM DESCRIPTION AND MODEL

A generic model is developed to demonstrate the concept and provide understanding of the integrated system. By assuming a uniform strain field in the host structure covered by the treatment and applying a globally stable self-sensing actuation control [1, 2], the deformation in the VEM layer and the hybrid constraining layer is derived. The loss factors of the system are then calculated to discuss the damping performance of the treatment.

The system studied is shown in Figure 1, where a beam is used as the one-dimensional host structure. The assumptions used to derive the model are: (1) The system is under longitudinal vibration with a uniform strain in the host structure. (2) The VEM layer is under shear deformation and system passive damping is only considered in the VEM. (3) Interfaces are perfect; no slip occurs between adjacent layers. (4) The displacement (δ) between the edge element location on the base beam and the corresponding end of the PZT layer is zero. (5) The applied voltage is assumed uniform along the PZT. (6) Only harmonic, steady state vibration is considered. (7) Linear theories of elasticity, viscoelasticity, and piezoelectricity are used.

Based on these assumptions, the equations of motion and corresponding boundary/connecting conditions governing the motion of the constraining layer can be derived as [10]

$$\frac{\partial^2 u_a}{\partial x^2} - \frac{G_v^*(u_a - u_b)}{E_a h_a h_v} = \frac{\rho_a}{E_a}\frac{\partial^2 u_a}{\partial t^2}, \quad 0 < x < \alpha L, \tag{1}$$

$$\frac{\partial^2 u_p}{\partial x^2} - \frac{G_v^*(u_p - u_b)}{E_p h_p h_v} = \frac{\rho_p}{E_p}\frac{\partial^2 u_p}{\partial t^2}, \quad \alpha L < x < L, \tag{2}$$

$$E_a h_a b\left(\frac{\partial u_a}{\partial x} - \Lambda\right) = K_{eq1}(u_a - u_b), \quad x = 0, \tag{3}$$

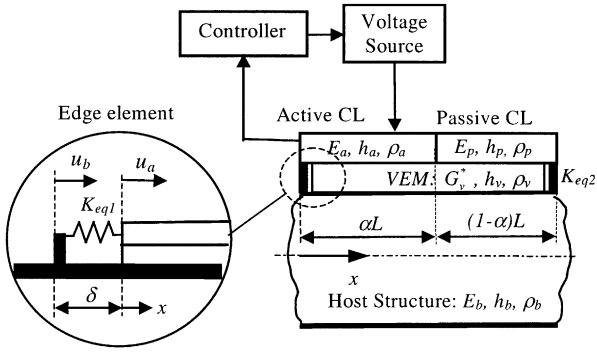

Figure 1. Combination of EACL and HCL.

$$E_p h_p b \frac{\partial u_p}{\partial x} = K_{eq2}(u_p - u_b), \quad x = L, \tag{4}$$

$$u_p = u_a, \qquad x = \alpha L, \tag{5}$$

$$E_a h_a \left(\frac{\partial u_a}{\partial x} - \Lambda \right) = E_p h_p \frac{\partial u_p}{\partial x}, \qquad x = \alpha L. \tag{6}$$

Here, subscripts a, p, v and b denote the quantities associated with the active constraining layer, the passive constraining layer, the VEM layer and the host beam respectively. E, h and ρ stand for Young's modulus, thickness and density of corresponding layers. G_v^* is the complex shear modulus of the VEM, which can be further expressed in terms of the material storage modulus (G_{v1}) and loss factor (η_v) as $G_{v1}(1 + i\eta_v)$. K_{eq1} and K_{eq2} are the equivalent longitudinal stiffness of the edge elements; Λ is the free strain of the active material; b is the width and L is the length of the treatment; α is the length ratio of the active material in the constraining layer (Figure 1).

Note that because of the longitudinal vibration assumption in the host structure, there is no transverse deformation in the system. This assumption thus significantly simplifies the mathematics involved while it still provides sufficient information for us to understand the characteristics of the damping treatment. In steady state, considering the separation of the variables in the forms of

$$u_b(x, t) = U_b(x)\mathrm{e}^{\mathrm{i}wt} \equiv \bar{U}_b(\bar{x})L\mathrm{e}^{\mathrm{i}wt}, \tag{7}$$

$$u_a(x, t) = U_a(x)\mathrm{e}^{\mathrm{i}wt} \equiv \bar{U}_a(\bar{x})L\mathrm{e}^{\mathrm{i}wt}, \tag{8}$$

$$u_p(x, t) = U_p(x)\mathrm{e}^{\mathrm{i}wt} \equiv \bar{U}_p(\bar{x})L\mathrm{e}^{\mathrm{i}wt}, \tag{9}$$

and assuming quasi-static of the system, equations (1)–(6) can be non-dimensionalized as

$$\frac{\mathrm{d}^2 \bar{U}_a}{\mathrm{d}\bar{x}^2} - \Gamma_a^2 \bar{U}_a = -\Gamma_a^2 \bar{U}_b, \quad 0 < \bar{x} < \alpha, \tag{10}$$

$$\frac{\mathrm{d}^2 \bar{U}_p}{\mathrm{d}\bar{x}^2} - \Gamma_p^2 \bar{U}_p = -\Gamma_p^2 \bar{U}_b, \quad \alpha < \bar{x} < 1, \tag{11}$$

$$\frac{\mathrm{d}\bar{U}_a}{\mathrm{d}\bar{x}} - \frac{\Lambda}{\mathrm{e}^{\mathrm{i}\omega t}} = K_1(\bar{U}_a - \bar{U}_b), \quad \bar{x} = 0, \tag{12}$$

$$\frac{\mathrm{d}\bar{U}_a}{\mathrm{d}\bar{x}} = -K_2(\bar{U}_p - \bar{U}_b), \quad \bar{x} = 1, \tag{13}$$

$$\bar{U}_p = \bar{U}_a, \quad \bar{x} = \alpha, \tag{14}$$

$$\frac{\mathrm{d}\bar{U}_a}{\mathrm{d}\bar{x}} - \frac{\Lambda}{\mathrm{e}^{\mathrm{i}\omega t}} = S_p \frac{\mathrm{d}\bar{U}_p}{\mathrm{d}\bar{x}}, \quad \bar{x} = \alpha, \tag{15}$$

where

$$\Gamma_p^2 = \frac{G_v^* L^2}{E_p h_p h_v}, \qquad \Gamma_a^2 = \frac{G_v^* L^2}{E_a h_a h_v}, \tag{16}$$

$$K_1 = \frac{K_{eq1} L}{E_a h_a b}, \qquad K_2 = \frac{K_{eq2} L}{E_a h_a b}, \tag{17}$$

$$S_p = \frac{E_p h_p}{E_a h_a} = \frac{\Gamma_a^2}{\Gamma_p^2}, \quad \bar{x} = x/L. \tag{18}$$

For a uniform strain field in the host structure covered by the treatment, the displacement in the beam can be expressed as

$$\bar{U}_b = c_0 + \varepsilon_0 \bar{x}, \tag{19}$$

where ε_0 is the assumed constant strain in the host structure and c_0 is an arbitrary constant, which has no effect on the treatment damping properties since it will be cancelled in the final loss factor expressions. For simplicity, c_0 is set to zero in this paper. The uniform strain distribution is general and valid for most applications, since the treatment length is usually much smaller than the wavelength of the vibration modes to be controlled.

Substituting equation (19) into equations (10) and (11), the general solutions to the equations of motion can be solved as

$$\bar{U}_a = A\cosh(\Gamma_a \bar{x}) + B\sinh(\Gamma_a \bar{x}) + \varepsilon_0 \bar{x} + c_0, \quad 0 < \bar{x} < \alpha, \tag{20}$$

$$\bar{U}_p = C\cosh(\Gamma_p \bar{x}) + D\sinh(\Gamma_p \bar{x}) + \varepsilon_0 \bar{x} + c_0, \quad \alpha < \bar{x} < 1. \tag{21}$$

The shear strain γ in the viscoelastic layer can be expressed as

$$\frac{\gamma}{e^{i\omega t}} = \begin{cases} \dfrac{\bar{U}_a - \bar{U}_b}{\theta_v} = \dfrac{A\cosh(\Gamma_a \bar{x}) + B\sinh(\Gamma_a \bar{x})}{\theta_v}, & 0 < \bar{x} < \alpha, \\ \dfrac{\bar{U}_p - \bar{U}_b}{\theta_v} = \dfrac{C\cosh(\Gamma_p \bar{x}) + D\sinh(\Gamma_p \bar{x})}{\theta_v}, & \alpha < \bar{x} < 1, \end{cases} \tag{22}$$

with

$$\theta_v = h_v/L. \tag{23}$$

Constants A, B, C and D can be found by substituting equations (19)–(21) into equations (12)–(15) with the replacement of the following self-sensing actuation algorithm [1, 2, 10, 11] for the free strain Λ,

$$\Lambda = iG[\bar{U}_a(0) - \bar{U}_a(\alpha)]e^{i\omega t}, \tag{24}$$

where G is the non-dimensional control gain.

The loss factors of the system are used as performance indices in this paper [10, 11]. The passive (η_p) and active (η_a) loss factors of the system are defined as

$$\eta_p = \frac{W_p}{2\pi W_s}, \qquad \eta_a = \frac{W_a}{2\pi W_s}, \tag{25, 26}$$

with

$$W_p = \pi \eta_v G_{v1} h_v b L \int_0^1 |\gamma|^2 \, d\bar{x}, \qquad W_a = \pi G E_a h_a b L |\bar{U}_a(0) - \bar{U}_a(\alpha)|^2, \tag{27, 28}$$

$$W_s = \frac{E_a h_a b L}{2}\left\{S_b \varepsilon_0^2 + K_1 |\bar{U}_a(0) - \bar{U}_b(0)|^2 + K_2 |\bar{U}_p(1) - \bar{U}_b(1)|^2 + \int_0^{\alpha} \left|\frac{\mathrm{d}\bar{U}_a}{\mathrm{d}\bar{x}}\right|^2 \mathrm{d}\bar{x} + S_p \int_{\alpha}^{1} \left|\frac{\mathrm{d}\bar{U}_p}{\mathrm{d}\bar{x}}\right|^2 \mathrm{d}\bar{x} + \mathrm{Re}[\Gamma_a^2]\theta_v^2 \int_0^1 |\gamma|^2 \,\mathrm{d}x\right\}, \tag{29}$$

$$S_b = \frac{E_b h_b}{E_a h_a}. \tag{30}$$

Here W_p is the energy dissipated per cycle through passive damping, W_a is the energy dissipated per cycle through active control and W_s is the maximum strain energy stored in the system.

Considering equations (27)–(29), the passive and active loss factors of the system can be represented by

$$\eta_p = \frac{\mathrm{Im}[\Gamma_a^2](I_1 + I_2)}{den}, \tag{31}$$

$$\eta_a = \frac{G|A - (A\cosh(\alpha\Gamma_a) + B\sinh(\alpha\Gamma_a) + \alpha\varepsilon_0)|^2}{den}, \tag{32}$$

where

$$den = S_b\varepsilon_0^2 + I_3 + S_p I_4 + \mathrm{Re}[\Gamma_a^2](I_1 + I_2) + K_1|A|^2 + K_2|C\cosh(\Gamma_p) + D\sinh(\Gamma_p)|^2, \tag{33}$$

$$I_1 = \int_0^{\alpha} |A\cosh(\Gamma_\alpha \bar{x}) + B\sinh(\Gamma_\alpha \bar{x})|^2 \,\mathrm{d}\bar{x}, \tag{34}$$

$$I_2 = \int_{\alpha}^{1} |C\cosh(\Gamma_p \bar{x}) + D\sinh(\Gamma_p \bar{x})|^2 \,\mathrm{d}\bar{x}, \tag{35}$$

$$I_3 = \int_0^{\alpha} |A\Gamma_\alpha \sinh(\Gamma_\alpha \bar{x}) + B\Gamma_\alpha \cosh(\Gamma_\alpha \bar{x}) + \varepsilon_0|^2 \,\mathrm{d}\bar{x}, \tag{36}$$

$$I_4 = \int_{\alpha}^{1} |C\Gamma_p \sinh(\Gamma_p \bar{x}) + D\Gamma_p \cosh(\Gamma_p \bar{x}) + \varepsilon_0|^2 \,\mathrm{d}\bar{x}. \tag{37}$$

The above integrations can be evaluated numerically or using the trigonometric identities of hyperbolic functions with complex arguments [12].

The active loss factor, η_a, reflects the direct active control authority of the piezoelectric layer on the host structure. The passive loss factor, η_p, reflects the passive damping ability of the VEM layer. For the closed-loop system ($G > 0$), this includes the open-loop damping of the baseline structure ($G = 0$) and the enhanced passive damping due to the additional VEM deformation induced by the active PZT action. The system total damping ability is the summation of the active and passive loss factors, which is defined as the closed-loop loss factor η_s. When the control gain G is zero (open-loop), η_a will be zero, and η_p will only contain passive damping of the baseline structure, which is defined to be the open-loop loss factor, η_{op}. The value of η_{op} reflects the fail-safe ability of the treatment.

4. OPTIMIZATION CASE STUDY

The focus of this paper is to evaluate the feasibility of integrating the EACL and HCL to provide better combination of the open-loop and closed-loop damping actions in the treatment. From the analysis given in the last section, the loss factors of the system are found to be related to seven independent parameters: Γ_a, S_p, K_1, K_2, G, α, and S_b. In this investigation, we will focus on the major parameters of the EACL (K_1 and K_2) and that of the HCL (α) as well as the self-sensing control gain (G). The nominal values for Γ_a, S_p and S_b are set to be $3{\cdot}28e^{i\pi/8}$, 6 and 10 respectively. Since there are still four independent parameters involved, instead of performing a lengthy parametric study, optimization techniques are used to find the optimal independent parameters (design variables) under different objective functions and constraint conditions. In summary, we have formed the following optimization problems:

Case 1 (Tables 1 and 2): Maximize $\eta_{op}(K_1, K_2, \alpha)$.

Other cases (Cases 2–10 in Table 1 and Cases 2–5 in Table 2):

$$\text{Maximize } \eta_s(K_1, K_2, \alpha, G), \quad \text{subject to: } \eta_{op}(K_1, K_2, \alpha) \geqslant \eta_{given}. \tag{38}$$

Here the open-loop loss factor (η_{op}) represents the system damping ability when the control gain G is zero. Other than Case 1, the objective function is to maximize the closed-loop loss factor (η_s) of the system. The loss factor constraint shown in equation (38) is to ensure that a minimum fail-safe damping (η_{given}) is maintained in the system. In addition to this damping constraint, the ranges and constraints of the design variables K_1, K_2, G, α are listed in Tables 1 and 2, which provide reasonable bounds for these parameters.

A method mixing a genetic (non-gradient based) algorithm [13] with a gradient-based scheme is utilized to search for the optimal design variables. Specifically, for the genetic algorithm, the MATLAB© subroutine of differential evolution (DE) for continuous function optimization developed by Price and Storn [*http://www.icsi.berkeley.edu/ ~ storn/code.html*] is used in this study. The advantage of utilizing such a genetic algorithm approach is that one can effectively avoid the local minimums. However, its convergence is very slow compared to a gradient-based optimization method, especially when the design variables are close to their optimal values. To compensate for the speed and precision, the DE algorithm is coupled with the gradient-based Sequential Quadratic Programming (SQP) scheme. The DE method is terminated after a given maximum number of iterations (generations) is reached. The results obtained from DE algorithm are then used as initial values for the SQP method implemented in MATLAB© optimization subroutine (*fminbnd*) so that the desired precision of the design variables can be achieved efficiently. By controlling the maximum number of iterations, the DE algorithm can be used to find an initial condition that is very close to the optimal value so that the gradient-based method will converge to the global minimum effectively. Results obtained using this methodology are presented in the next few paragraphs and the physics behind the results are explained in the next section.

To examine the maximum open-loop damping ability of the integrated system, an unconstrained optimization for maximizing the open-loop loss factor of the integrated system is first performed (Case 1 of Table 1). The final optimal design is a PCL treatment with an edge element at one end.

Cases 2–10 in Table 1 list the optimal values of the design variables and the corresponding loss factors for nine different requirements of the open-loop damping. Case 2 presents the maximum possible closed-loop damping of such a system. It ends up with a symmetric EACL design with the stiffest (highest value in the given range) edge elements. The open-loop damping of such a design is almost zero. Cases 3–10 provide the

TABLE 1

Optimal design variables and loss factors for the integrated system

#	Objective function	Constraints on η_{op}	η_{op}	η_p	η_a	η_s	Design variables			
							$0 \leqslant K_1 \leqslant 100$	$0 \leqslant K_2 \leqslant 100$	$0 \leqslant \alpha \leqslant 1$	$0 \leqslant G \leqslant 100$
1	η_{op}	None	0·078	0·078	0	0·078	100 (0)	0 (100)	0	0
2	η_s	None	$1{\cdot}7 \times 10^{-5}$	0·004	0·958	0·962	100	100	1	22·1
3	η_s	$\eta_{op} \geqslant 0{\cdot}005$	0·005	0·014	0·409	0·423	100	100	0·734	12·5
4	η_s	$\eta_{op} \geqslant 0{\cdot}01$	0·01	0·015	0·306	0·321	100	100	0·612	11·3
5	η_s	$\eta_{op} \geqslant 0{\cdot}015$	0·015	0·015	0·230	0·245	100	100	0·492	10·7
6	η_s	$\eta_{op} \geqslant 0{\cdot}018$	0·018	0·014	0·182	0·195	100	100	0·396	10·5
7	η_s	$\eta_{op} \geqslant 0{\cdot}019$	0·019	0·012	0·160	0·175	56·8	100	0·372	9·88
8	η_s	$\eta_{op} \geqslant 0{\cdot}0195$	0·0195	0·012	0·150	0·162	39·8	100	0·372	9·36
9	η_s	$\eta_{op} \geqslant 0{\cdot}02$	0·02	0·040	0·116	0·156	100	0	0·511	26·7
10	η_s	$\eta_{op} \geqslant 0{\cdot}025$	0·025	0·039	0·106	0·145	100	0	0·414	26·4

TABLE 2

Optimal design variables and loss factors for EACL

#	Objective function	Constraint on η_{op}	η_{op}	η_p	η_a	η_s	Design variables		
							$0 \leqslant K_1 \leqslant 100$	$0 \leqslant K_2 \leqslant 100$	$0 \leqslant G \leqslant 100$
1	η_{op}	None	0·0168	0·0168	0	0·0168	0	0	0
2	η_s	None	$1{\cdot}7 \times 10^{-5}$	0·004	0·958	0·962	100	100	22·1
3	η_s	$\eta_{op} \geqslant 0{\cdot}005$	0·005	0·051	0·091	0·142	100 (1·57)	1·57(100)	6·29
4	η_s	$\eta_{op} \geqslant 0{\cdot}01$	0·01	0·069	0·043	0·112	100 (0·121)	0·121 (100)	7·755
5	η_s	$\eta_{op} \geqslant 0{\cdot}015$	0·015	0·041	0·008	0·0487	0·451 (0)	0 (0·451)	8·081

optimal design variables and corresponding loss factors when the requirement for the open-loop damping is gradually increased. Note from Table 1 that when the required open-loop loss factor is not very high, say $\eta_{given} \leqslant 0{\cdot}018$(Cases 2–6), the optimization ends up with a treatment with an active–passive hybrid constraining layer and two stiffest edge elements. This indicates that designing an active–passive hybrid constraining layer is a better approach to provide fail-safe damping than reducing the stiffness of the edge elements. With further increase of the fail-safe requirement, the stiffness of one edge element has to be reduced also to satisfy the constraint as shown in Cases 7–10. It can also be observed from Table 1 that the closed-loop damping decreases with the increase of open-loop damping.

The non-unity optimal values of the active material coverage ratio shown in Table 1 imply that implementing an active–passive hybrid constraining layer in an EACL treatment (integrating the HCL and EACL) provides a means to achieve a better mixture between the open-loop and closed-loop damping. Table 2 lists the optimal design parameters and the corresponding loss factors for the first five cases when the active material coverage ratio is set to 1 (pure EACL). Because the constraining layer has to be a piezoelectric layer, the maximum open-loop damping that an EACL system can achieve is less than that of the integrated system (compare Case 1 in Tables 1 and 2). When some fail-safe damping is required in the system (Cases 3–5), the stiffness of one edge element has to be reduced. Note that the total system damping of these EACL designs are less than that of the combined designs when the same amount of fail-safe damping is required. This phenomenon suggests that combining HCL into the EACL design, one can obtain the required fail-safe damping with less reduction on the closed-loop damping, as compared to only reducing the EACL edge element stiffness.

5. PHYSICAL EXPLANATION OF THE OPTIMIZATION RESULTS

The optimization results presented in the last section demonstrated that it is beneficial to combine EACL and HCL. The phenomenon is related to the fact that considerable shear

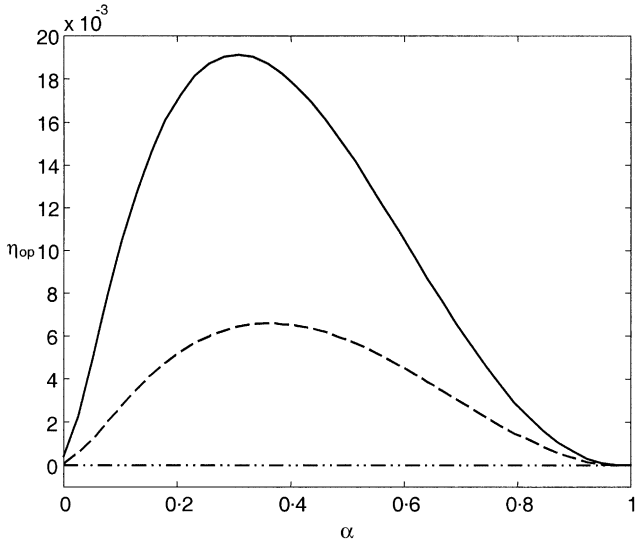

Figure 2. *Open*-loop loss factor versus active material coverage ratio ($K_1 = K_2 = 100$); – · · – · · – –, $S_p = 1$; – – – – –, $S_p = 3$; ———, $S_p = 6$.

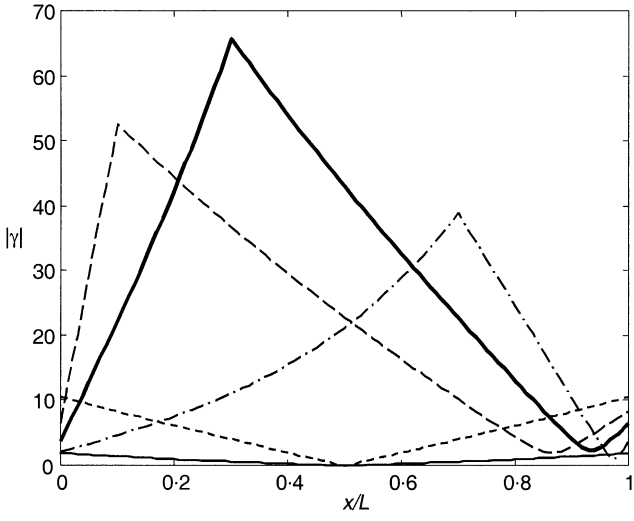

Figure 3. Shear strain distribution in the VEM layer ($K_1 = K_2 = 100$, $\varepsilon_0 = 1$): - - - - -, $\alpha = 0$; – – – – –, $\alpha = 0{\cdot}1$; ——, $\alpha = 0{\cdot}3$; – · – · –, $\alpha = 0{\cdot}7$; ——, $\alpha = 1$.

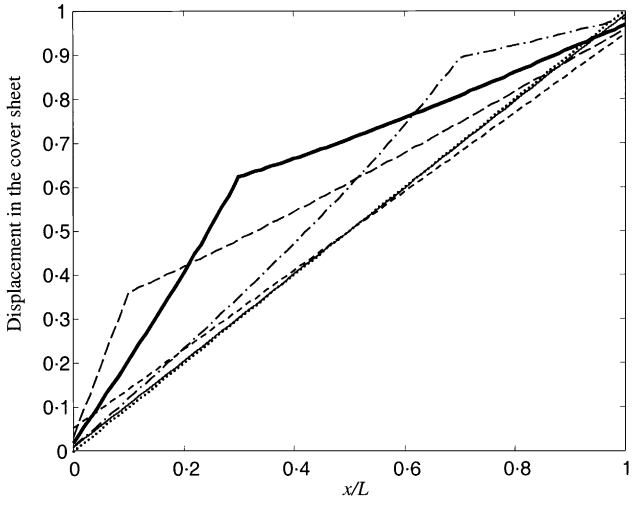

Figure 4. Longitudinal displacement in the constraining layer and host beam ($K_1 = K_2 = 100$, $\varepsilon_0 = 1$): - - - - -, $\alpha = 0$; – – – – –, $\alpha = 0{\cdot}1$; ——, $\alpha = 0{\cdot}3$; – · – · –, $\alpha = 0{\cdot}7$; ——, $\alpha = 1$; ·····, displacement in the host beam.

can be generated in the viscoelastic layer by the hybrid constraining layer even when both edge elements are designed to be stiff.

Figure 2 illustrates the effects of the active material coverage ratio (α) and the extensional stiffness ratio between the passive and active constraining materials (S_p) on the open-loop loss factor (η_{op}) of the treatment. The non-dimensionalized edge element stiffness used in the figure is 100. Compared to the HCL treatment without edge elements or with one edge element [10, 12], a very distinguished difference is that the treatment here does NOT obtain the maximum open-loop damping when the cover sheet is completely made of passive materials ($\alpha = 0$), although a larger S_p still provides better damping in general. In fact, an optimal active material coverage ratio exists even for the open-loop system.

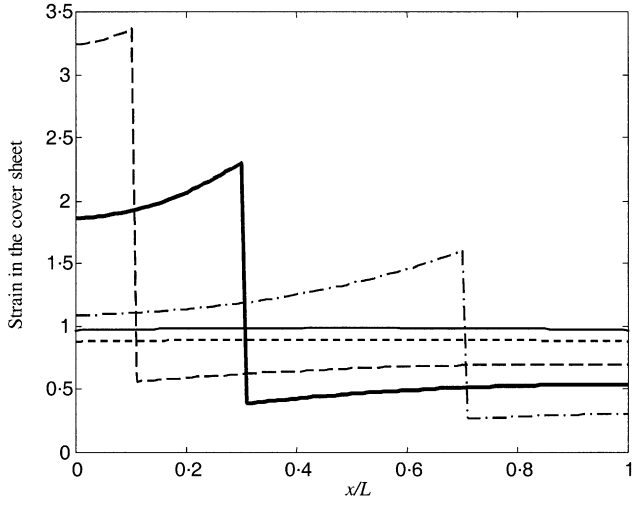

Figure 5. Longitudinal strain distribution in the constraining layer ($K_1 = K_2 = 100$, $\varepsilon_0 = 1$): - - - - -, $\alpha = 0$; – – – – –, $\alpha = 0{\cdot}1$; ——, $\alpha = 0{\cdot}3$; –·–·–·, $\alpha = 0{\cdot}7$; ——, $\alpha = 1$.

Figure 3 shows the shear strain distribution in the viscoelastic layer for different selections of the active material coverage ratio in the open-loop system. Clearly, stiffer constraining layer creates larger shear deformation in the viscoelastic layer ($\alpha = 0$ versus $\alpha = 1$). However, when a hybrid constraining layer is used, the shear in the viscoelastic layer can be even greater than that when the constraining layer is purely passive. Specifically, significant shear strain can be generated for $\alpha = 0{\cdot}3$, which explains the peak open-loop loss factor in Figure 2.

The shear distribution pattern shown in Figure 3 is related to the longitudinal displacements of the constraining layer and the host structure, which are shown in Figure 4 for different α values. According to equation (22), the shear in the viscoelastic layer is proportional to the difference of the displacements in the cover sheet and the host structure. The extensional stiffness discrepancy between the active and passive constraining materials generates a discontinuity of the longitudinal strain in the constraining layer as indicated in Figure 5. Therefore, considerable displacement difference is created between the host structure and the constraining layer in the middle section of the treatment.

Based on these observations, an ACL treatment can be improved by (a) adding equal and stiff edge elements (symmetric EACL) to ensure high closed-loop damping, and (b) using the hybrid constraining cover sheet to increase the open-loop loss factor and guarantee sufficient fail-safe damping, as illustrated by the optimization results shown in Cases 3–6 in Table 1.

The maximum open-loop damping for the treatment with two stiff edge elements shown in Figure 2 is the highest fail-safe damping that such a system can provide. If the required fail-safe damping is higher, such as in Cases 7–10 in Table 1, the stiffness of the edge elements has to be reduced. Note that for these cases, the pure EACL design cannot satisfy the fail-safe damping requirement even when the edge element stiffness is reduced to zero (Case 1 in Table 2). Therefore, the integration of the EACL and HCL not only provides a better combination between the open-loop and closed-loop damping, but also broadens the hybrid damping ability of the EACL or HCL.

6. CONCLUSIONS

The damping ability of the integrated EACL and HCL treatment is investigated in this paper. An optimization problem and an analysis process are developed to derive the design variables for the integrated system and provide understanding of the characteristics of this new treatment. The design is to maximize the closed-loop damping performance while maintaining a fail-safe damping margin in the system.

It is demonstrated in this study that the integration of EACL and HCL can obtain a better combination of the open-loop and closed-loop damping. When the required fail-safe damping is not very high, a design with two stiff and equal edge elements and an active–passive hybrid constraining layer can be used to satisfy the fail-safe damping requirement and achieve significant closed-loop damping. A close examination of the design reveals that the difference of the extensional stiffness of the active and passive constraining sections creates large shear deformation in the middle section of the viscoelastic material, although the shear at the boundaries is small. The stiff edge elements in the mean time will increase the active control action from the constraining layer. Consequently, the closed-loop damping of such a design is higher than that of an EACL treatment when the same amount of fail-safe damping is obtained through reducing the edge element stiffness.

When the required fail-safe damping is relatively high, the design with two stiff and equal edge elements and an active–passive hybrid constraining layer cannot provide enough open-loop damping. The stiffness of one edge element has to be reduced to meet the fail-safe requirement. In this case, the pure EACL design alone cannot provide enough fail-safe damping. HCL, although it can achieve the required fail-safe damping, will provide less closed-loop damping. Therefore, the integration of the EACL and HCL actually broadens the damping ability of the individual EACL or HCL design.

ACKNOWLEDGMENTS

This research is supported by the U.S. Army Research Office, with Dr. Gary Anderson as the technical monitor.

REFERENCES

1. A. BAZ 1997 *Smart Materials and Structures* **6**, 360–368. Optimization of energy dissipation characteristics of active constrained layer damping.
2. I. Y. SHEN 1997 *American Society of Mechanical Engineers, Journal of Vibration and Acoustics* **119**, 192–199. A variational formulation, a work-energy relation and damping mechanisms of active constrained layer treatments.
3. W. H. LIAO and K. W. WANG 1997 *American Society of Mechanical Engineers, Journal of Vibration and Acoustics* **119**, 563–572. On the active–passive hybrid control actions of active constrained layers.
4. A. BAZ and J. RO 1995 *Journal of Mechanical Design* (*Special 50th Anniversary Design Issue*) **117**, 135–144. Optimum design and control of active constrained layer damping.
5. M. C. RAY and A. BAZ 1997 *Journal of Sound and Vibration* **208**, 391–406. Optimization of energy dissipation of active constrained layer damping treatments of plates.
6. W. C. VAN NOSTRAND and D. J. INMAN 1995 in *Proceedings of SPIE on Active Materials and Smart Structures*, San Diego, CA, Vol. 2427, 124–139. Finite element model for active constrained layer damping.
7. W. H. LIAO and K. W. WANG 1996 *Smart Materials and Structures* **5**, 638–648. A new active constrained layer configuration with enhanced boundary actions.
8. M. J. LAM, D. J. INMAN and W. R. SAUNDERS 1997 *Journal of Intelligent Material Systems and Structures* **8**, 663–677. Vibration control through passive constrained layer damping and active control.

9. M. J. LAM, D. J. INMAN and W. R. SAUNDERS 1998 in *Proceedings of SPIE on Smart Structures and Materials*, San Diego, CA, Vol. 3327, 32–43. Variations of hybrid damping.
10. Y. LIU and K. W. WANG 2000 *American Society of Mechanical Engineers, Journal of Vibration and Acoustics* **122**, 254–262. Active–passive hybrid constrained layer for structural damping augmentation.
11. Y. LIU and K. W. WANG 1999 *Journal of Sound and Vibration* **223**, 611–644. A non-dimensional parametric study of enhanced active constrained layer damping treatments.
12. Y. LIU and K. W. WANG 1999 in *Proceedings of the* 1999 *ASME Design Engineering Technical Conferences*, Las Vegas, NV, DETC/VIB-8301. Surface damping treatment with an active–passive hybrid constraining layer.
13. S. S. RAO 1996 *Engineering Optimization*: *Theory and Practice*. New York: John Wiley & Sons.